RESEARCH ARTICLE

Multi-Class Kidney Abnormalities Detecting Novel System Through Computed Tomography

SAGAR DHANRAJ PANDE[ID] AND RAGHAV AGARWAL[ID]

School of Computer Science and Engineering (SCOPE), VIT-AP University, Amaravati, Andhra Pradesh 522237, India

Corresponding author: Sagar Dhanraj Pande (sagar.pande@vitap.ac.in)

ABSTRACT Impaired renal function poses a risk across all age groups. Because of the global shortage of nephrologists, the growing public health concern over renal failure, and technological improvements, there is a demand for an AI-driven system capable of autonomously detecting kidney abnormalities. Chronic kidney disease, commonly known as chronic renal failure, is characterized by a progressive decline in kidney function. Renal failure can be caused by a variety of reasons, including cysts, stones, and tumors. Chronic kidney disease may not have apparent symptoms at first, resulting in instances staying untreated until they reach an advanced state. Tumors are dense clumps of tissue that can cause direct injury to glands, spinal cells, and other organs. The presence of a substantial number of solids in the digestive tract causes kidney stone disease, also known as urolithiasis. This study used a deep learning model to detect kidney illnesses to solve the global scarcity of urologists. The project entailed obtaining and annotating a large dataset of 12,446 CT whole abdomen and urogram images, with an emphasis on kidney stones, cysts, and tumors, which are the most common types of renal illness. The dataset was divided into four categories: cyst, tumor, stone, and normal. Data was collected from several hospitals in the Dhaka area. This work presents an innovative and customizable platform for the clinical diagnosis of kidney diseases such as tumors, stones, and cysts. Our YOLOv8 model's enhanced accuracy opens up new possibilities for identifying kidney cysts, stones, and tumors. We used criteria like accuracy, precision, recall, F1 score, and specificity to evaluate its performance. The network attained an accuracy rate of 82.52%, 85.76% precision, 75.28% recall, 75.72% F1 score, and 93.12% specificity.

INDEX TERMS Kidney pathology, stone, tumor, cysts kidney diseases, computed tomography.

I. INTRODUCTION

Despite continued attempts to combat kidney disease, its prevalence continues to be a major public health problem [1]. Chronic kidney disease affects more than 10% of the world's population [2] and was the 16th largest cause of death in 2016. Alarmingly, forecasts show that it will rise to sixth place by 2040 [3]. In 2020, around 79,000 people in the United States were diagnosed with kidney cancer, with 28,710 cases in women and 50,290 cases in males [4], [5]. An estimated 431,288 cases of kidney cancer were

The associate editor coordinating the review of this manuscript and approving it for publication was Wuliang Yin[ID].

recorded worldwide [4], [5]. It's worth noting that kidney cancer is the sixth most prevalent malignancy among men in the United States. Nephrolithiasis, cyst development, and renal cell carcinoma (kidney tumor) are examples of primary kidney disorders that impact renal function. In the United States, around 6% of women and 11% of men have had kidney stones at some point in their life [6], [7]. Men are more likely than women to acquire kidney stones, and people with a family history of kidney stones are also at a higher risk. Furthermore, people with a history of kidney stones frequently have repeating occurrences. Dehydration is another factor that contributes to the production of kidney stones.

Individuals of all ages commonly have kidney-related problems. However, manually spotting these anomalies may be costly, time-consuming, and difficult. As a result, medical research has concentrated on developing a quick and reliable approach to identifying renal diseases. Kidney stone disease, which is characterized by the production of crystalline deposits within the kidneys, affects around 12% of the world's population [8]. Renal cell carcinoma (RCC), often known as kidney tumor, is one of the top 10 malignancies with the highest incidence rates in the world [9]. RCC develops when kidney cells undergo aberrant alterations and uncontrolled proliferation, ultimately leading to kidney cancer. Among the most frequent signs of kidney cancer are flank discomfort, elevated blood pressure, and blood in the urine. Some kidney tumors are deemed benign and pose no risk. Non-cancerous growths, in contrast to malignant tumors, are often smaller in size and do not metastasize, which means they do not spread to other areas of the body. As a tumor develops in size, the likelihood that it is benign rises. Larger tumors, on the other hand, are more likely to be cancerous or malignant.

Kidney cysts are fluid-filled sacs that can form on the surface or inside the kidneys. These cysts are linked to disorders that can influence both renal and blood function. The most frequent variety is a simple kidney cyst, which is usually innocuous and causes no problems. Isolated kidney cysts are rather common. Multiple cysts in one or both kidneys, on the other hand, might cause difficulties. Differentiating between simple cysts and polycystic kidney disease is critical. Cysts are classified as simple or complicated. Complex cysts must be closely watched for any changes that might suggest malignancy.

Pathology tests are usually used in conjunction with other imaging modalities to identify renal issues, such as X-rays, computed tomography (CT), B-ultrasound devices (US), and MRIs. CT scanners use X-ray beams to generate comprehensive cross-sectional pictures of the targeted anatomy, resulting in exact slice-by-slice images and three-dimensional data, making them useful instruments in kidney research [10]. Early detection and treatment of kidney abnormalities such as cysts, stones, and tumors are critical in avoiding renal failure [11]. As a result, early diagnosis of renal illnesses such as kidney cysts, stones, and tumors is seen as a key first step in preventing kidney failure [12].

The fast development of sophisticated MRI scanners and other cutting-edge medical imaging modalities has boosted the demand for computer-aided diagnostic tools. At the moment, healthcare experts must methodically analyze complicated medical pictures to find problems, which is a difficult and time-consuming process. There is an increasing demand for systems that can recognize organs autonomously, detect probable anomalies, and deliver vital information to reduce the load on clinicians and improve diagnostic efficiency.

The use of an artificial intelligence (AI) model to detect kidney-related radiological results quickly has considerable promise for assisting healthcare practitioners and decreasing patient suffering. Given the frequency of renal disorders,

the global scarcity of nephrologists and radiologists, and advances in deep learning research for visual tasks, this is extremely important.

Furthermore, it is critical to recognize that tumors can directly injure certain organs such as glands and spinal cells. Despite recent research, the availability of public datasets remains fairly limited. Previously, typical machine learning algorithms were used to categorize diseases including cysts, tumors, and stones. Ultrasonography scans were used as part of the study approach in several investigations.

This research has made numerous significant contributions, including:

1. The collection "CT Kidney Dataset: Normal-Cyst-Tumor and Stone" was created and annotated, consisting of 12,446 pictures of the complete abdomen collected using the Eurogram method.
2. Implementation of a YOLOv8-based deep learning model for the identification of renal diseases. The study paper includes a full performance analysis as well as a detailed description of the suggested technique's underlying mechanics.
3. The performance of the YOLOv8 model is evaluated by analyzing several variables derived from the confusion matrix, such as precision, recall, accuracy, specificity, and F1 score. These numbers clearly show the model's capacity to detect and diagnose renal diseases.

The remainder of the paper is divided into the following sections. Section II includes research background information. Section III discusses the methodology used in this investigation, as well as the model and data-gathering procedures. Section IV discusses the assessment methodology as well as the findings of the study. Section V finishes the article by making a conclusion and some future recommendations.

II. RELATED WORK

This section provides a detailed summary of early renal research from diverse angles. Deep learning's application in image processing and classification has resulted in a substantial body of study, notably in the field of self-diagnosis of radiological results.

For the categorization of renal disorders, several deep-learning techniques have been investigated. In one study, researchers compared convolutional neural networks (CNNs) to traditional machine learning techniques such as decision trees (DTs), random forests (RFs), support vector machines (SVMs), multilayer perceptrons (MLPs), K-nearest neighbors (KNNs), naive Bayes, and others [13]. The authors earned the highest F1 score of 0.853 among the numerous ways, suggesting the efficiency of their methodology.

To extract information from renal ultrasound pictures, the authors of [14] used pre-trained Deep Neural Network (DNN) models such as ResNet-101, ShufeNet, and MobileNet-v2. The collected characteristics were then categorized using Support Vector Machines (SVM), and the final predictions were generated using the majority vote approach. The study's

major emphasis was ultrasound image categorization, which achieved an excellent accuracy of 95.58%.

A mix of classic and deep transfer learning approaches was used in a separate investigation by the authors of [15]. Using the SVM Classifier, they used ultrasound picture features to distinguish between normal and abnormal ultrasound images. This method demonstrated the use of transfer learning in the interpretation of ultrasound pictures.

The authors reported a method for the automatic detection of kidney stones using deep learning algorithms and coronal Computed Tomography (CT) images [16]. Their proposed approach has an astounding detection accuracy of 96.82%. For training and assessing the model, a dataset of 1,799 photos was used.

Similarly, the authors of [17] created a technique for identifying kidney cyst pictures using abdominal CT scan data. For this challenge, they used a fully connected Convolutional Neural Network (CNN) and attained a true-positive rate of 84.3%.

The authors of [18] modified the ResNet-101 model by adding a $1 \times 1 \times 1$ convolution layer with initialized weights and altering the final dense layer to accommodate categorization into five unique classes. The proposed design has a 95% average confidence interval and an AUC of 0.88. The model's accuracy rating was 0.72.

Reference [19] focused on categorizing renal ultrasonography pictures into five categories: tumor, cyst, normal, stone, and failure. The authors used Principal Component Analysis (PCA) to determine the most important characteristics from a small number of variables. These selected characteristics were then used to train a neural network, yielding an amazing 97% accuracy.

In conclusion, prior attempts to use machine learning and deep learning algorithms to identify specific renal radiographic abnormalities have yielded encouraging results. However, the majority of these efforts have been focused on the analysis of X-ray or ultrasound pictures. Dual-class categorization has gotten little attention, particularly in the context of CT scan pictures. Our study tries to close this gap by categorizing CT images into four unique categories.

III. PROPOSED WORK

The goal of this study is to investigate the use of YOLOv8 in the identification of renal diseases utilizing CT scans. The purpose of this research is to employ the YOLOv8 technique to undertake in-depth categorization of renal disorders. Unlike traditional convolutional networks, which take numerous passes and significant CPU resources to analyze an image, the unique You Only Look Once (YOLO) architecture was used in this study to classify kidney diseases. The YOLO object identification method uses neural networks to recognize things in a single pass. The suggested classification approach seeks to uncover differentiating traits that classify various renal illnesses. Before sending the kidney to the classifiers, the system locates, identifies, and correctly

places it to permit further analysis. The hyperparameter of our YOLOv8n-cls model is given in Table 1.

TABLE 1. Hyperparameter given to proposed YOLOv8-cls.

Hyperparameter	Value
Epochs	50
Batch	16
Imgsz	128
Conf	0.25
IOU	0.7

Using widely available photos, the trained system exhibits the capacity to detect kidney abnormalities even in difficult settings. The improved YOLOv8 network detects objects of varying sizes and resolutions with surprising resiliency. It has a high level of classification accuracy, especially when it comes to renal illnesses, and operates well in difficult conditions. Figure 1 depicts the proposed method for using YOLO in the categorization of renal disorders.
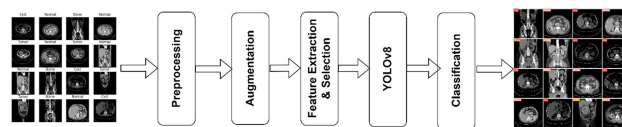

FIGURE 1. Proposed framework.

A. DATA ACQUISITION

To achieve our main goal, we gathered a big dataset of kidney photos depicting diverse illnesses. This collection contains images of various situations such as cysts, tumors, stones, and normal kidney states. Using the Picture Archiving and Communication System (PACS), data was collected from different hospitals in Dhaka, Bangladesh. Patients have previously been diagnosed with kidney stones, cysts, tumors, or normal renal diseases at these hospitals [20]. We intentionally chose Coronal and Axial slices from both contrast and non-contrast exams during complete abdominal and urogram operations to create our dataset (see Figure 2). To assure the dataset's accuracy, the acquired data was thoroughly scrutinized, including significant cross-referencing and painstaking verification utilizing numerous websites. The training dataset was carefully selected to provide a varied spectrum of complete datasets. There are a total of 12,446 photos in the collection, which have been divided into four separate categories. The training dataset contains 9,957 pictures, which account for almost 80% of the whole dataset. Furthermore, the validation dataset contains 2,489 photos, accounting for roughly 20% of the whole dataset (see Table 2). This divide enables a distinct set of data to evaluate the model's performance as well as an acceptable number of samples to train the model properly.

The dataset used in this work is made up of a huge number of labeled photos or video frames, each of which contains
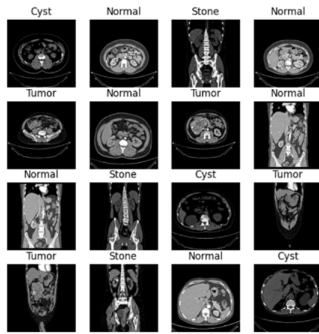
FIGURE 2. Sample representation of the dataset.

TABLE 2. Dataset distribution.

	Cyst	Normal	Stone	Tumor	Images per Split
Train	2967	4062	1102	1826	9957
Test	742	1015	275	457	2489
Images per class	3709	5077	1377	2283	

information about the species depicted. Backgrounds, lighting conditions, and angles vary in these images. A balanced dataset method is used to guarantee that the YOLOv8 model is trained to reliably recognize all target species without bias towards overrepresented classes. This method enhances fairness during training by guaranteeing that each class in the dataset has an equal number of images. After training the YOLOv8 model with the training set, the validation set is utilized to evaluate the system's performance. It gives vital insights into the model's overall performance and allows for the evaluation of its efficacy using previously overlooked data.

B. PRE-PROCESSING
Images or video frames are frequently pre-processed before being supplied into the object identification model to overcome distortions and differences in lighting conditions. This step of image processing includes scaling, grayscale conversion, pixel value normalization, and the use of picture-enhancing methods such as histogram equalization or contrast stretching. These pre-processing processes guarantee that the input picture or video frame is in an acceptable format for future processing and, if necessary, has been scaled to fit the YOLOv8 input size. You may guarantee that the input data is properly prepared for subsequent analysis by conducting these pre-processing procedures.

C. DATA AUGMENTATION
When opposed to starting from scratch, using pre-trained deep learning models that were originally built on large-scale, general-purpose datasets like ImageNet and fine-tuning them on a renal dataset can provide better results. The level of improvement, however, is determined by several criteria, including the quantity and quality of the renal dataset,

the model's design, and the specific job being handled. Using the original training data, this method comprises training and changing the model. This technique can yield excellent results if the first training dataset is sufficiently vast and diverse, including the variability inherent in renal pictures. If the training dataset is short or lacking in variety, the model may struggle to handle picture variances and may fail to generalize to new data adequately.

We use data augmentation techniques in this work to enhance the training data and increase the number of training instances. This entails modifying the raw photos, such as flipping, rotating, resizing, and adding noise. Using the enhanced training data, the model is then fine-tuned. Our goal is to improve the model's performance and resilience by using a more diversified and enlarged dataset. When presented with fresh and previously unexplored data, the model can acquire more robust features and display greater generalization skills by including data augmentation.

D. FEATURE EXTRACTION AND SELECTION
The method of feature extraction is used to decrease the quantity of information in huge datasets by choosing and merging key variables while rejecting less significant ones. Before completing feature extraction, it is critical to carefully select acceptable features, since these features have a substantial influence on the quality of neural network models. Image categorization relies heavily on feature extraction and selection. The initial training data used to build the model acts as a guide for feature selection. The approach evaluates the selected features as well as the metadata throughout the classification process to discover sets of learning algorithm parameters with favourable attributes. These chosen characteristics are then utilized to build a model and train the classification algorithm.

E. APPLIED YOLOV8N-CLS MODEL
The YOLOv8-cls object classification architecture uses a single convolutional neural network (CNN) to conduct classification in a single forward pass. Because of its quick inference time, this architecture is well-suited for real-time applications. The performance of the system is determined by several criteria, including the quantity and quality of the training data, as well as the complexity of the renal illnesses being identified.

The YOLOv8-cls system is an enhanced and more precise version of the original YOLOv8 system. It gives image classification algorithms a constant training environment. Ultralytics released the newest member of the YOLO family in 2023, which includes deep-learning algorithms for object detection and picture segmentation.

F. FULL-FLEDGED WORKING ON YOLO MODELS
The obtained kidney picture is sent into the system, where it is preprocessed to highlight key characteristics and remove distracting aspects. The YOLO method is then used to segment the picture, taking the region of interest into account.

Color, shape, and texture attributes are taken from these segments. To determine the presence or absence of an ailment, a convolutional neural network (CNN) is used.

For example, in the case of a picture exhibiting a bacterially diseased kidney, the image is split into numerous grids. Each grid predicts a set of bounding boxes, allowing objects to be identified within each grid cell. The image's height and breadth are defined by its total size, whereas the center coordinates of each cell are always known.

A bounding box is used in image analysis to emphasize the important parts of an item based on the expected class probabilities for each grid cell. In our example, we trained the model particularly on the sick area of the kidney, as shown by another bounding box, to enable prediction of the disease's dimensions (height, breadth, and center).

There are two types of bounding boxes at work. The first box depicts the degree of the disease by focusing just on the ill region of the kidney. The second box depicts the whole bounding box of the kidney. The IOU measure is used to calculate the amount to which these two boxes overlap. By using the IOU, YOLO generates an output box that correctly encloses the items of interest, ensuring perfect delineation.

Individual predictions are combined to get the final detection findings. The algorithm chooses the most likely class and assigns it to the grid cell linked with renal diseases. The algorithm proceeds as follows:

Step 1: The input picture is grid-divided, and each grid cell generates bounding box predictions as well as confidence ratings.

Step 2: The grid cells compute the probability for several classes to identify the class of the item.

Step 3: Using the IOU metric, any superfluous bounding boxes that do not match the properties of the item are removed.

Step 4: Separate boundary boxes are used in the final detection step to identify and localize kidney abnormalities.

Given that the kidney is always the major focus, the algorithm shifts the emphasis of the bounding box from the entire kidney to the specific condition under consideration. This improvement improves the algorithm's capacity to identify renal problems properly. After completing the preceding phases successfully, the YOLO approach works as expected, providing the necessary vector that offers exact information about the bounding box associated with the appropriate class.

G. OBJECTIVE OF USING YOLOV8

The suggested approach for categorizing renal irregularities intends to standardize and automate kidney abnormality monitoring. It is feasible to get insights into the distribution and frequency of various kidney illnesses by identifying and categorizing renal abnormalities. This information is critical for patient health conservation, management, and comprehension. Computer vision approaches provide a more precise and consistent classification of kidney problems than previous

methods. Furthermore, in this context, computer vision offers faster and more efficient data processing. The subject of renal abnormalities identification and classification is fast advancing due to the continual innovation of new technology. To progress the discipline and get a better grasp of renal classification, researchers are continually investigating and creating novel algorithms and methodologies. While deep learning approaches have made tremendous progress in the diagnosis and categorization of renal illnesses, there are still important research gaps that must be addressed. Many existing deep-learning models for categorizing renal illnesses are computationally demanding and may not be suited for real-time applications. Models must be concise and efficient to be deployed on systems with limited computing resources. By resolving these issues, we may create kidney categorization systems that are more user-friendly and practical.

IV. RESULTS AND DISCUSSION
A. EXPERIMENTAL SETUP
This entire project was trained using a system that met the following criteria: AMD Ryzen 7 5800H has a Radeon graphics processor clocked at 3.20 GHz. Our test configuration included a 512 GB SSD, a 64-bit operating system, and 16 GB of RAM. The computational workloads were handled by an NVIDIA RTX 3050 GPU in the study.

B. EVALUATION METRICS
The parameters of the assessment model, such as accuracy, precision, recall, specificity, and F1 score, have been established.

(a) Accuracy: The model's performance is measured by its accuracy, which is calculated by comparing the ratio of true positives and true negatives to all past forecasts.

$$\text{Accuracy}_i : (TP_i + TN_i)/(TP_i + TN_i + FP_i + FN_i) \quad (1)$$

(a) Precision: The true positive rate, which represents the percentage of accurately predicted positive cases out of all instances predicted, is used to assess the model's accuracy. This statistic evaluates the accuracy of the model's predictions.

$$\text{Precision}_i = TP_i/(TP_i + FP_i) \quad (2)$$

(b) Recall: The model calculates the number of real positive values, which are occurrences of positivity that were accurately detected and tallied as such. This metric represents the model's ability to recognize affirmative cases reliably.

$$\text{Recall}_i = TP_i/(TP_i + FN_i) \quad (3)$$

(c) Specificity: The capacity of the system to detect negative outcomes reliably is measured by measuring the proportion of negative cases that are appropriately labeled as negative. This statistic assesses the system's

ability to effectively recognize and categorize negative situations.

$$Specificity_i = TN_i/(TN_i + FP_i) \quad (4)$$

(d) F1-score: When there is a trade-off between accuracy and recall scores and there is a worry about high false positive or false negative rates, the F1 score is used. It acts as a harmonic means of precision and recollection, assisting in the balance of accuracy and recall. The F1 score aids in the construction of an appropriate balance between these two measures, to achieve a balanced measure that takes both precision and recall into account.

$$F1 - score_i$$
$$= 2(Precision_i * Recall_i)/(Precision_i + Recall_i) \quad (5)$$

where,

• i = For the categorization challenge, choose Kidney Tumour, Cyst, Normal, or Stone.

• True Positive (TP): The patient is unwell, and the model predicts a favorable outcome.

• True Negative (TN): The patient is not sick, and the model forecasts the same.

• False Positive (FP): The patient is healthy, and the model's prediction is right.

• False Negative (FN): The patient has the illness, yet the test results are negative.

C. PERFORMANCE EVALUATION

This part discusses the findings. The deep learning model's loss and accuracy, as shown in Figure 3, are crucial because they give a measurable evaluation of the model's performance for a specific job. The loss function evaluates the model's ability to minimize the difference between predicted and actual results. A lower loss number suggests that the model predicts more accurately. Furthermore, the accuracy indicator displays the model's percentage of true predictions. When comparing numerous models and picking the best one for a certain job, analyzing the loss and accuracy of a deep learning
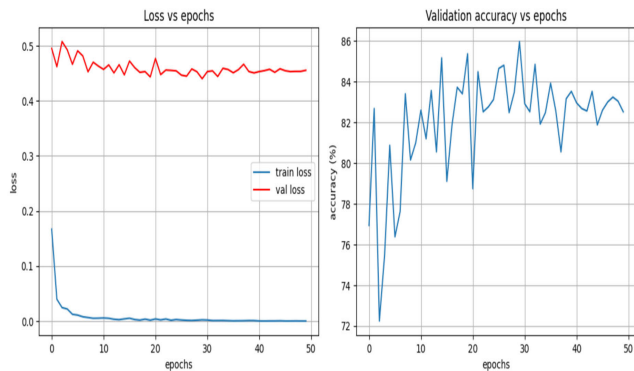
TABLE 3. Performance evaluation by several metrics.

	Accuracy	Precision	Sensitivity/Recall	Specificity	F1-score
Cyst	97.23	98.41	92.18	99.37	95.19
Normal	86.34	74.90	100	76.93	85.65
Stone	94.46	73.22	78.54	96.43	75.78
Tumor	87.02	96.52	30.41	99.75	46.25
Overall	82.52	85.76	75.28	93.12	75.72

model is critical. It not only aids in the evaluation of the model's performance, but it also detects whether the model is overfitting or underfitting the training dataset, signaling the need for further fine-tuning. Table 4 displays the training results for each epoch, providing detailed information about the model's performance and evolution through time. This in-depth examination offers a better grasp of how the model works and grows during training.

The confusion matrix, as shown in Figure 4, is a popular technique for assessing the performance of a deep learning-based image classification model. For each class in the dataset, this matrix gives thorough information on true positives, false positives, true negatives, and false negatives. It is calculated by comparing the predicted and actual class labels of a series of test photos used for renal disease classification. The confusion matrix provides useful information about the model's performance, especially in circumstances with several classes. It enables an assessment of how well the deep learning model recognizes each class. This study aids in comprehending the model's strengths and flaws in detecting renal diseases. The confusion matrix is a useful tool for assessing the overall performance of a deep learning-based image classification model and finding specific classes that the network has difficulty distinguishing. It gives insights into areas where focused training enhancements may be required to overcome these difficulties. As a result, the confusion matrix is an important tool for evaluating the performance of such models, providing a thorough study of accuracy and suggesting possible areas for further development. Table 3 shows the expected outcomes for the proposed YOLOv8 model, allowing for a thorough analysis of its performance across several classes.
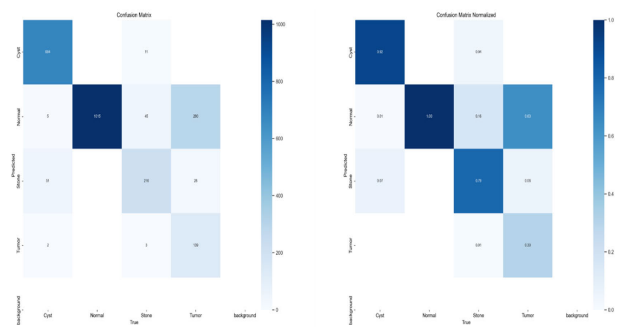

FIGURE 3. Loss and accuracy evaluation graph.

FIGURE 4. Obtained confusion matrix for YOLOv8n-cls.

TABLE 4. Training results per epochs.

Epochs	train/loss	metrics/accuracy_top1	metrics/accuracy_top5	val/loss	lr/pg0	lr/pg1	lr/pg2
1	0.16683	0.76939	1	0.49482	0.000238	0.000238	0.000238
2	0.03963	0.82684	1	0.46161	0.000466	0.000466	0.000466
3	0.0245	0.72238	1	0.50736	0.000685	0.000685	0.000685
4	0.02195	0.75452	1	0.49236	0.000672	0.000672	0.000672
5	0.01232	0.80876	1	0.46598	0.000672	0.000672	0.000672
6	0.01085	0.76376	1	0.49055	0.000657	0.000657	0.000657
7	0.00783	0.77622	1	0.48117	0.000643	0.000643	0.000643
8	0.00646	0.83407	1	0.45239	0.000629	0.000629	0.000629
9	0.00504	0.80153	1	0.46982	0.000615	0.000615	0.000615
10	0.00527	0.80996	1	0.46277	0.000601	0.000601	0.000601
11	0.00564	0.82603	1	0.45679	0.000587	0.000587	0.000587
12	0.00508	0.81197	1	0.46492	0.000573	0.000573	0.000573
13	0.00334	0.83568	1	0.4504	0.000558	0.000558	0.000558
14	0.00261	0.80554	1	0.46532	0.000544	0.000544	0.000544
15	0.00399	0.85175	1	0.44685	0.00053	0.00053	0.00053
16	0.0052	0.79108	1	0.47192	0.000516	0.000516	0.000516
17	0.00283	0.8188	1	0.45998	0.000502	0.000502	0.000502
18	0.00181	0.83728	1	0.45142	0.000488	0.000488	0.000488
19	0.00359	0.83407	1	0.45281	0.000474	0.000474	0.000474
20	0.00173	0.85376	1	0.44311	0.00046	0.00046	0.00046
21	0.00387	0.78746	1	0.47654	0.000445	0.000445	0.000445
22	0.00222	0.84492	1	0.4473	0.000431	0.000431	0.000431
23	0.0038	0.82523	1	0.45561	0.000417	0.000417	0.000417
24	0.00152	0.82764	1	0.45499	0.000403	0.000403	0.000403
25	0.00285	0.83126	1	0.45408	0.000389	0.000389	0.000389
26	0.00197	0.84652	1	0.44634	0.000375	0.000375	0.000375
27	0.00141	0.84813	1	0.44448	0.000361	0.000361	0.000361
28	0.00112	0.82483	1	0.45759	0.000346	0.000346	0.000346
29	0.00164	0.83487	1	0.45251	0.000332	0.000332	0.000332
30	0.00227	0.85978	1	0.43979	0.000318	0.000318	0.000318
31	0.00195	0.82925	1	0.45285	0.000304	0.000304	0.000304
32	0.00094	0.82523	1	0.45412	0.00029	0.00029	0.00029
33	0.00098	0.84853	1	0.44388	0.000276	0.000276	0.000276
34	0.00108	0.8192	1	0.45878	0.000262	0.000262	0.000262
35	0.00073	0.82483	1	0.45653	0.000247	0.000247	0.000247
36	0.00044	0.83929	1	0.45064	0.000233	0.000233	0.000233
37	0.00057	0.82563	1	0.45643	0.000219	0.000219	0.000219
38	0.00065	0.80554	1	0.46615	0.000205	0.000205	0.000205
39	0.00095	0.83166	1	0.45289	0.000191	0.000191	0.000191
40	0.00087	0.83528	1	0.4504	0.000177	0.000177	0.000177
41	0.00024	0.82965	1	0.45282	0.000163	0.000163	0.000163
42	0.00015	0.82684	1	0.45454	0.000149	0.000149	0.000149
43	0.00028	0.82563	1	0.45701	0.000134	0.000134	0.000134

TABLE 5. *(Continued.)* Training results per epochs.

44	0.00028	0.83528	1		0.45144	0.00012	0.00012	0.00012
45	0.00049	0.8188	1		0.45789	0.000106	0.000106	0.000106
46	0.00016	0.82603	1		0.45437	9.20E-05	9.20E-05	9.20E-05
47	0.00017	0.83005	1		0.45279	7.78E-05	7.78E-05	7.78E-05
48	0.00029	0.83246	1		0.45315	6.37E-05	6.37E-05	6.37E-05
49	0.00019	0.83045	1		0.45318	4.96E-05	4.96E-05	4.96E-05
50	0.00019	0.82523	1		0.4552	3.54E-05	3.54E-05	3.54E-05

V. CONCLUSION AND FUTURE REMARKS

During the implementation phase, a multi-class classification strategy is used to categorize various renal illnesses. When a picture is supplied, the deep learning-based YOLOv8n-cls model is used to identify various sorts of illnesses. In real-world applications, this model is useful since it can recognize newly discovered illness categories that were incorporated during the training phase. This technique provides a unique solution in the field and supports disease control management by making it easier to identify and categorize relevant diseases [21].

Ultralytics created the sophisticated object categorization algorithm YOLOv8n-cls. A convolutional neural network (CNN) at the heart of this technique does image processing in a single pass, providing predicted class labels for each item in the picture. Based on the input picture, the method's architecture consists of an object categorization detection head and an image feature extraction backbone network. The YOLOv8n-cls framework successfully classifies objects thanks to its economical technique.

According to our findings, the YOLOv8n-cls algorithm detects numerous kidney illnesses with a high degree of confidence and in a fair period. The algorithm's success within the limits of the experiment demonstrates its efficacy. Future developments may make use of newer forms of YOLO to improve on the existing design. Furthermore, the pre-trained YOLOv8n-cls model, which is well-known for its speed and accuracy in object classification tasks, may be used in mobile apps, particularly on small-screen phones for which it has been optimized.

REFERENCES

[1] S. Jacobson, "Chronic kidney disease public health problem?" *Lakartidningen*, vol. 110, no. 21, pp. 1018–1020, 2013.

[2] V. Jha, G. Garcia-Garcia, K. Iseki, Z. Li, S. Naicker, B. Plattner, R. Saran, A. Y.-M. Wang, and C.-W. Yang, "Chronic kidney disease: Global dimension and perspectives," *Lancet*, vol. 382, no. 9888, pp. 260–272, Jul. 2013.

[3] K. J. Foreman et al., "Forecasting life expectancy, years of life lost, and all-cause and cause-specific mortality for 250 causes of death: Reference and alternative scenarios for 2016–40 for 195 countries and territories," *Lancet*, vol. 392, no. 10159, pp. 2052–2090, 2018.

[4] S. Sudharson and P. Kokil, "Computer-aided diagnosis system for the classification of multi-class kidney abnormalities in the noisy ultrasound images," *Comput. Methods Programs Biomed.*, vol. 205, Jun. 2021, Art. no. 106071.

[5] Y. Huo, Z. Xu, S. Bao, A. Assad, R. G. Abramson, and B. A. Landman, "Adversarial synthesis learning enables segmentation without target modality ground truth," in *Proc. IEEE 15th Int. Symp. Biomed. Imag. (ISBI)*, Apr. 2018, pp. 1217–1220.

[6] N. Hadjiyski, "Kidney cancer staging: Deep learning neural network based approach," in *Proc. Int. Conf. E-Health Bioeng. (EHB)*, Oct. 2020, pp. 1–4.

[7] I. Castiglioni, L. Rundo, M. Codari, G. Di Leo, C. Salvatore, M. Interlenghi, F. Gallivanone, A. Cozzi, N. C. D'Amico, and F. Sardanelli, "AI applications to medical images: From machine learning to deep learning," *Phys. Medica*, vol. 83, pp. 9–24, Mar. 2021.

[8] T. Alelign and B. Petros, "Kidney stone disease: An update on current concepts," *Adv. Urol.*, vol. 2018, pp. 1–12, May 2018.

[9] J. J. Hsieh, M. P. Purdue, S. Signoretti, C. Swanton, L. Albiges, M. Schmidinger, D. Y. Heng, J. Larkin, and V. Ficarra, "Renal cell carcinoma," *Nature Rev. Disease Primers*, vol. 3, no. 1, pp. 1–19, 2017.

[10] K. C. Saw, J. A. McAteer, A. G. Monga, G. T. Chua, J. E. Lingeman, and J. C. Williams, "Helical CT of urinary calculi: Effect of stone composition, stone size, and scan collimation," *Amer. J. Roentgenol.*, vol. 175, no. 2, pp. 329–332, Aug. 2000.

[11] T. D. K. S. C. Gunasekara, P. M. C. S. De Silva, E. M. D. V. Ekanayake, W. A. K. G. Thakshila, R. A. I. Pinipa, P. M. M. A. Sandamini, S. D. Gunarathna, E. P. S. Chandana, S. S. Jayasinghe, C. Herath, S. Siribaddana, and N. Jayasundara, "Urinary biomarkers indicate pediatric renal injury among rural farming communities in Sri Lanka," *Sci. Rep.*, vol. 12, no. 1, pp. 1–13, May 2022.

[12] Y. Bi, X. Shi, J. Ren, M. Yi, and X. Han, "Transarterial chemoembolization of unresectable renal cell carcinoma with doxorubicin-loaded CalliSpheres drug-eluting beads," *Sci. Rep.*, vol. 12, no. 1, pp. 1–8, May 2022.

[13] I. Aksakalli, S. Kaçdioğlu, and Y. S. Hanay, "Kidney X-ray images classification using machine learning and deep learning methods," *Balkan J. Electr. Comput. Eng.*, vol. 9, no. 2, pp. 144–151, Apr. 2021.

[14] S. Sudharson and P. Kokil, "An ensemble of deep neural networks for kidney ultrasound image classification," *Comput. Methods Programs Biomed.*, vol. 197, Dec. 2020, Art. no. 105709.

[15] Q. Zheng, S. L. Furth, G. E. Tasian, and Y. Fan, "Computer-aided diagnosis of congenital abnormalities of the kidney and urinary tract in children based on ultrasound imaging data by integrating texture image features and deep transfer learning image features," *J. Pediatric Urol.*, vol. 15, no. 1, pp. 75.e1–75.e7, Feb. 2019.

[16] K. Yildirim, P. G. Bozdag, M. Talo, O. Yildirim, M. Karabatak, and U. R. Acharya, "Deep learning model for automated kidney stone detection using coronal CT images," *Comput. Biol. Med.*, vol. 135, Aug. 2021, Art. no. 104569.

[17] N. Blau, E. Klang, N. Kiryati, M. Amitai, O. Portnoy, and A. Mayer, "Fully automatic detection of renal cysts in abdominal CT scans," *Int. J. Comput. Assist. Radiol. Surg.*, vol. 13, no. 7, pp. 957–966, Jul. 2018.

[18] K.-H. Uhm, S.-W. Jung, M. H. Choi, H.-K. Shin, J.-I. Yoo, S. W. Oh, J. Y. Kim, H. G. Kim, Y. J. Lee, S. Y. Youn, S.-H. Hong, and S.-J. Ko, "Deep learning for end-to-end kidney cancer diagnosis on multi-phase abdominal computed tomography," *NPJ Precis. Oncol.*, vol. 5, no. 1, p. 54, Jun. 2021, doi: 10.1038/s41698-021-00195-y.

[19] M. Wagih, F. E. Z. Abou-Chadi, H. El-Din, and N. Mekky, "Classification of ultrasound kidney images using PCA and neural networks," *Int. J. Adv. Comput. Sci. Appl.*, vol. 6, no. 4, 2015.

[20] M. Islam. (2021). *CT Kidney Dataset: Normal-Cyst-Tumor and Stone*. [Online]. Available: https://www.kaggle.com/nazmul0087/ct-kidney-dataset-normal-cyst-tumor-and-stone

[21] R. Agarwal and D. Godavarthi, ''Skin disease classification using CNN algorithms,'' *EAI Endorsed Trans. Pervasive Health Technol.*, vol. 9, Oct. 2023, doi: 10.4108/eetpht.9.4039.

SAGAR DHANRAJ PANDE received the Ph.D. degree in computer science and engineering from Lovely Professional University, Phagwara, Punjab, India, in 2021. He is currently an Assistant Professor Senior Grade with VIT-AP University, Amaravati, Andhra Pradesh, India. He has published and presented more than 80 articles in Springer, Elsevier, CRC, Taylor & Francis, and other reputable journals which are Scopus indexed and peer-reviewed journals. Also, he has published more than 30 patents on the topics of data mining, network security, the IoT, and their application. Also, he has published papers at international conferences Springer on the topics of data mining, network security, the IoT, and their application. He has supervised several postgraduate students in cybersecurity, computer networks, communication, and the IoT. He is responsible for teaching artificial intelligence, deep learning, machine learning, cyber crime and security, and Python programming courses to undergraduate and postgraduate students. His research interests include deep learning, machine learning, network attacks, cyber security, and the Internet of Medical Things (IoMT). He received the Emerging Scientist Award from the VDGOOD Professional Association, in 2021, and the Young Researcher Award and the Best Ph.D. Thesis Award from Universal Innovators, in 2022.

RAGHAV AGARWAL received the B.Tech. degree in computer science from VIT-AP University, Andhra Pradesh. He worked on different technical and research-focused projects. He has published more than two patents on healthcare along with many SCI journals and conferences during his graduation. Beyond the classroom, he regularly engages in research programs across the world that are relevant to his area of interest including AI/ML and data science.

● ● ●